HHS Public Access

Author manuscript

Cell Tissue Res. Author manuscript; available in PMC 2017 March 01.

Published in final edited form as:

Cell Tissue Res. 2016 March ; 363(3): 791–803. doi:10.1007/s00441-015-2273-x.

A POPULATION OF MITOCHONDRION-RICH CELLS IN PARS RECTA OF MOUSE KIDNEY

M. S. Forbes, **B. A. Thornhill**, **C. I. Galarreta**, and **R. L. Chevalier**

Division of Pediatric Nephrology Department of Pediatrics University of Virginia School of Medicine Charlottesville, VA 22908, USA

Abstract

Following perfusion of adult mouse kidney with a solution of nitroblue tetrazolium (NBT), certain epithelial cells in the pars recta (S3) segments of proximal tubules react to form cytoplasmic deposits of blue diformazan particles. Such cells are characterized by dark cytoplasm, small and often elliptical nuclei, elaborate, process-bearing profiles, and abundant mitochondria. The atypical epithelial cells display the additional characteristic of immunoreactivity for a wide spectrum of antigens, including mesenchymal proteins such as vimentin. Though present in kidneys of untreated or sham-operated animals, they are particularly evident under experimental conditions such as unilateral ureteral obstruction (UUO), appearing in both contralateral and obstructed kidneys over the course of a week's duration, but disappearing from the obstructed kidney as it undergoes the profound atrophy attributable to deterioration of the population of its proximal tubules. The cells do not appear in neonatal kidneys, even those undergoing UUO, but begin to be recognizable soon after weaning (28 days). It is possible that diformazan-positive cells in the mouse S3 tubular segment constitute a resident population of cells that can replenish or augment the tubule. Although somewhat similar cells, with dark cytoplasm and vimentin expression, have been described in human, rat, and transgenic mouse kidney (Smeets et al., 2013; Berger et al., 2014), those cells—known as “scattered tubule cells” or “proximal tubule rare cells” differ from the S3-specific cells in that they are present throughout the entire proximal tubule, often lack a brush border, and have only few mitochondria.

Keywords

Mouse kidney; UUO; proximal tubule; mitochondria; stem cells; progenitor cells

INTRODUCTION

Acute kidney injury and chronic kidney disease are major causes of morbidity and mortality, and are characterized by progressive nephron loss resulting from tubular and interstitial injury (Chawla et al., 2014). It has long been known that the kidney is capable of reparative ability under a variety of conditions (Romagnani, 2013). The basis for regeneration has been debated over the past decade, and has been attributed to a wide variety of phenomena, among them epithelial-to-mesenchymal transformation or EMT, in which tubule cells become phenotypically altered in order to generate replacement cells. Alternatively, it has long been proposed that cells from outside the kidney (notably bone marrow-derived) are attracted to the sites of injury and there become epithelial cells. This last scenario has,

however, been disputed on the basis of elegant lineage-tracing experiments (Duffield and Humphreys, 2011). Kidney-resident cells of the papilla, of blood vessels, of capsule, or within the glomerulus have also been postulated as sources of regenerative cells. EMT itself appears to be falling out of favor, insofar as being a process of reversion in which epithelial cells completely leave the tubule; for example, resident fibroblasts themselves are now thought to be the source of myofibroblasts (Picard et al., 2008). The tide in fact appears to be turning toward the view of resident tubule cells being both sufficient in number and capable in capacity to undergo mitosis in response to injury to their fellows. The question of note now involves whether such cells undergo division while maintaining their differentiated phenotype (Vogetseder et al., 2007, 2008) or first undergo “dedifferentiation” before dividing and subsequently regaining their polarized morphology. Fujigaki et al. (2009) indicate that in fact either condition can prevail, depending on the degree of injury.

Surgical unilateral ureteral obstruction (UUO) is the most widely used animal model of chronic kidney disease (Chevalier et al., 2009), and has provided the basis for many of the above-referenced reports. In the course of our studies on the UUO model in mice (Forbes et al., 2011, 2013), we discovered a population of cells within the S3/pars recta segment of the proximal tubules which were distinguishable because of their staining affinity following perfusion with nitroblue tetrazolium (NBT), a technique designed to reveal sites of production of reactive oxygen species (ROS). We observed that in normal mouse kidney there is preferential disposition of the reduced tetrazole (diformazan) around the nephron components possessing the most mitochondria, namely the proximal-tubule epithelial cells (Forbes et al., 2011). Under conditions of UUO, however, the proximal tubules of the obstructed kidney undergo considerable deterioration from the combined effects of apoptosis, necrosis and autophagy, the last serving to concentrate diformazan within autophagosomes, indicating that defunct mitochondria and their generated ROS are thereby sequestered. Surface-associated diformazan is lost from these atrophic tubules, likely from the loss of the majority of functional mitochondria.

These cells of mouse pars recta are similar in certain respects to populations found scattered throughout proximal tubules in human and diseased rat (Smeets et al., 2013), which have been proposed as candidates for supporting regeneration. We elected to make further study of the mouse cells, to establish their structural, chemical and morphometric parameters, the better to understand their potential role in mouse kidney.

MATERIALS AND METHODS

Male C57B/6 mice ranging from 14 days to 6 weeks of age were used for this study. In additional adult (>6 wk) male mice of the C57Bl strain, complete unilateral ureteral obstruction (UUO) was performed as previously described (Forbes et al., 2011, 2013), and their kidneys were examined 3, 7 or 14 days post-obstruction. Untreated or sham-operated animals of similar age were used as controls. A total of 25 mice were used in this study.

Mitochondrial activity that generates reactive oxygen species can be detected in renal tissue by the administration through the vasculature of nitroblue tetrazolium (NBT; Chien et al., 2001). Following their technique, we have found that the reduction of the colorless tetrazole

results in its conversion to blue diformazan crystals, which are typically deposited at the basal surfaces of the tall epithelial cells of the proximal tubule and its derivatives, the proximal-tubule epithelium-like cells that typically form part of the glomerular capsule (Forbes et al., 2011).

This procedure entailed a 1-minute transcardial perfusion (rate of 7 ml/min) with Hank's balanced salt solution (HBSS), followed by a 1-minute perfusion of 1 mg/ml nitroblue tetrazolium (Sigma N5514) in HBSS, followed by another minute of washout perfusion with HBSS. For paraffin embedment, kidneys were fixed in phosphate-buffered formalin solution, or, for plastic embedment, the perfusion was continued with 2.5% glutaraldehyde in HBSS, with additional immersion in glutaraldehyde fixative. Paraffin embedments were cut at thicknesses ranging from 2-10 μm and counterstained with 1% Neutral Red or periodic-acid Schiff (PAS)-hematoxylin. For the preparation of semithin and ultrathin plastic sections, glutaraldehyde-perfused kidneys were cut into 50 μm sections with a vibrating microtome (D.S.K Microslicer DTK-3000, Ted Pella, Redding CA). These sections were examined in fresh-cut form to confirm NBT staining, and selected sections containing diformazan deposits were processed either with or without osmication, then dehydrated and infiltrated with Poly/Bed 812 resin (Polybed, Inc., Warrington, PA), after which they were affixed to microscope slides and cured at 60°C as previously described (Forbes et al., 2002); regions were then selected for cutting on Sorvall MT-2B or Leica Ultracut EM UC7 ultramicrotomes. Both semithin (ca. 0.25 μm) sections and ultrathin (70-90 nm) sections were prepared. Semithin sections were lightly counterstained with 1% basic fuchsin in 50% ethanol or 1% toluidine blue in sodium borate. Light microscopy was performed with a Leica DMLS compound microscope (Leica Microsystems, Wetzlar, Germany) equipped with a QColor 3 digital camera (Olympus Corp. Valley, PA), and photographs were prepared with Adobe Photoshop v. 7.0. Ultrathin sections were stained on grid with uranyl acetate and lead citrate and examined in a JEOL 1230 transmission electron microscope.

Further characterization of pars recta cells was made in sections of NBT-perfused kidney stained with biotinylated *Lotus tetragonolobus* agglutinin (Vector Laboratories # B-1325, Burlingame CA), which strongly stains the apical cytoplasm of definitive epithelial cells of mouse proximal tubules (Forbes et al., 2011). A similar staining pattern results from megalin immunostaining, which like *Lotus* is localized in the apical tubulovesicular system (Birn et al., 2002; Nagai et al., 2005; Mahadevappa et al., 2013). Given the possibility that these cells represent a population of stem cells, additional histochemical and immunohistochemical staining of both NBT-perfused and conventionally (formalin)-fixed tissue was undertaken, testing antibodies against a variety of antibodies, including vimentin, α-SMA, nestin, CD-44, LSD-1, etc. , as well as TUNEL staining to test for apoptosis (details of suppliers, catalog numbers, and staining procedures are listed in Table 1).

Since the original recognition of the cells was made in the contralateral kidneys of 14-day UUO mice, median sagittal sections of 6 such mice that had been perfused with NBT were prepared; for each, one section was counterstained with neutral red, and another immunostained for vimentin (counting of cells in which diformazan and vimentin immunostaining were colocalized was not attempted, both because of the difficulty in distinguishing diformazan against the DAB background and the clearly greater incidence of

vimentin-stained cells). The numbers of diformazan-positive cells in one section were tallied and compared with the vimentin-positive cells in the other.

RESULTS

The changes in kidney structure in adult mouse subjected to unilateral ureteral obstruction (UUO) are characterized by the development of hydronephrosis in the ipsilateral kidney and compensatory growth of the contralateral kidney (Fig. 1). Whereas little structural change is seen in contralateral kidneys (Fig. 1b, cf. Fig. 1a), rapid loss of proximal-tubule mass is seen in obstructed kidneys after 7 days of obstruction (Fig. 1c), with severe renal atrophy evident after 14 days (Fig. 1d).

In normal or contralateral mouse kidneys perfused with nitroblue tetrazolium (NBT) (Fig. 2), the S1 and S2 segments of proximal tubules show dense deposition of blue diformazan crystals on their outer (basal) surfaces (Fig. 2a). In contrast, diformazan staining in the S3 portions of the proximal tubules (a.k.a. pars recta) is concentrated within individual cells (Fig. 2 a-d). Detailed inspection of such cells shows that they differ structurally from adjacent columnar epithelial cells; their selective staining with diformazan demonstrates irregular cell shapes that in certain planes of section are triangular or even stellate, rather than columnar and cylindrical as the majority of epithelial cells. Their nuclei, in addition, frequently are smaller, elliptical or fusiform in profile, and largely heterochromatic, again in contrast to conventional epithelial cells, which typically contain large spherical nuclei that are basally-located and euchromatic (Fig. 2 c-h). Examination of semithin plastic-embedded sections (Fig. 2i-k) confirms the presence of these cells, their cytoplasmic content of diformazan crystals, and their atypical morphology.

First noted in contralateral kidneys of UUO animals, the cells are also initially present in obstructed kidneys, until the progressive deterioration typical of ureteral ligation brings about disappearance of the S3 segments there. These unusual cells are also found in unoperated and sham-operated kidneys. Extreme variations in shape are found among cells in the same kidney, including “ganging” of multiple confluent cells (Fig. 3a, b). In some instances, individual cells appear to be binucleate (Fig. 3b. c), an impression further supported by examination of semithin (<0.25 μm) plastic sections (Fig. 3d).

Vimentin immunostaining has been shown in putative stem cells, with strong positivity observed in populations within rat and human proximal tubules (Smeets et al., 2013). It was therefore not surprising that the mouse cells were clearly stained against this mesenchymal protein (Fig. 4a). Less predicted was the finding that though many vimentin-positive cells were also diformazan-positive, this was not always the case (Fig. 4b). Furthermore, doublets of cells, one vimentin-positive and the other diformazan-stained, could sometimes be found (Fig. 4c, d).

Having noted a disparity between vimentin immunostaining and diformazan deposition, we compared serial sections to establish their relationship in contralateral and obstructed kidneys in six 14-day UUO mice. In the contralateral kidneys, vimentin-positive cells outnumbered those that were diformazan-stained, (respective averages per section of

352:191 = a ratio of 1.84:1). In the obstructed kidneys of these animals, a much lower incidence of these cells was seen overall, with the ratio being nearly equal (11.33:11.67 = 1.03:1). In obstructed kidneys, though the cells could be identified after 3 days of UUO, progressively fewer examples appeared at 7 days, and they had largely disappeared by 14 days, a phenomenon presumably attributable to the substantial loss of the S3 segments from multiple forms of cell death (Forbes et al., 2011).

Two markers of proximal tubular epithelial cell maturation were studied as well: *Lotus tetragonolobus* lectin affinity and megalin immunostaining. In the case of *Lotus* staining, examples of apical lectin negativity (Fig. 4e) and positivity (Fig. 4f) could be identified in diformazan-bearing cells. In contrast, diformazan-stained cells consistently lacked an apical megalin signal (Fig. 4g), and only developed one in the absence of diformazan deposition (Fig. 4h).

The cells displayed intense osmiophilia in plastic-embedded material that had been processed with a postfixation step (Fig. 5). In semithin sections, on the basis of their opaque cytoplasts, the cells could be readily identified, ranging in form from stellate profiles with small nuclei (Fig. 5a) through cells whose volume and nuclear size increased (Fig. 5b-d), to columnar entities that, while retaining their opacity, occupied the entire wall thickness of the proximal tubule and closely resembled adjacent proximal tubular epithelial cells (Fig. 5e, f).

In the electron microscope (Fig.6), the basis for cytoplasmic opacity was revealed to be a product of the combination of an abundance of large mitochondria that occupy the majority of the cytoplast (Fig. 6a-d) and ribosomes, both cytoplasmic and membrane-bound (Fig. 6c). Consistent with light-microscopic observations, the nuclei were often smaller and more heterochromatic than those of proximal tubular epithelial cells (Fig. 6b). Cells corresponding to the spectrum indicated in Fig. 5 shared the property of mitochondrial abundance. Those that had become columnar also displayed a distinct apical junctional complex and a developed tubulovesicular complex (Fig. 6e,f); the presence of the latter would correspond to the staining for Lotus lectin and megalin seen in some cells (Fig. 6f, 4h).

Although cells with diformazan-filled cytoplasm are most obvious in the pars recta, other examples were found as well in the NBT-perfused mouse kidney. These included cells having a dendritic appearance, but located within medullary tubules (Fig.7a-c), apparently those of the loop of Henle (Fig. 7d). Occasional diformazan-positive cells are found in the interstitium (Fig. 7e) and some profiles suggest attachment to the tubule periphery, with a process penetrating between the epithelial cells of the tubule wall (Fig. 7f).

DISCUSSION

Certain cells in mouse nephrons interact with NBT that has been introduced by vascular perfusion, resulting in deposition of blue diformazan crystals within their cytoplasm. These cells are found primarily in walls of the pars recta segment of proximal tubules. In these cells, a spectrum of cell shapes can be identified that suggests a progression from a polymorphic, perhaps primitive stage up to definitive proximal tubule epithelial cells. The varied shapes of the cells, as well as their small, eccentric, dark nuclei indicates that there is

some intrinsic modification that exists—in some cells, to some degree—at all times in the adult animal: this is supported by a low level of diformazan-positive cells that can be discerned as early as 28 days of age, both in some unoperated animals and in contralateral kidneys under conditions of UUO. By this time the kidneys have taken on all the morphological appearance of fully adult mouse kidneys. It is at this age, under conditions of UUO, that the obstructed kidneys fall prey to the various degenerative conditions—loss of patent glomerulotubular junctions and occurrence of autophagy in fragmented proximal tubules--that are present in adult mice with obstructed kidneys (Forbes et al., 2013).

A well-understood, but seldom expressed tenet that applies to the majority of applications of biological microscopy is the pitfall implicit in the rendering of dynamic conclusions on the basis of observations made on static entities ("histological snap shots") (Duffield and Humphreys, 2011). With this proviso in mind, we offer the hypothesis that the mitochondrion-rich cells in the mouse S3 tubular segment constitute a resident population of cells that can replenish or augment the tubule in response to growth or injury. The various forms taken by the cells fall into a spectrum that strongly suggests a developmental sequence whereby, *mutatis mutandis*, they become fully-differentiated proximal tubular epithelial cells. That these forms represent a single cell type is supported by the substantial mitochondrial content uniformly observed in the electron microscope. Additional features common to diformazan-positive S3 segment and S1 segment proximal tubular epithelial cells include the presence of a brush border and the apical tubulovesicular system (Fig. 6).

Progressive differentiation of diformazan-positive S3 segment cells is indicated by the observation of cells that not only exhibit profiles that range from stellate to columnar, but also by correlation of the columnar form with an apical staining pattern with either *Lotus* lectin or megalin antibody. Affinity for both ligands is associated with the presence of the endocytic (tubulovesicular) system that is typically present in definitive, structurally-polarized proximal tubular epithelial cells, there likely involved with the shuttling of materials (particularly carbohydrates, since *Lotus* lectin is specific for α-L-fucose: Hanae et al., 1994) between the apical cell surface and the Golgi apparatus. An additional observation in the pars recta is the appearance of "doublets" of these cells (Fig. 4c, d), resembling the pattern associated with stem cells (Maeshima et al., 2003; Challen et al., 2006), in which sets of daughter cells are present, some of which can differentiate into conventional epithelium for the purposes of normal or compensatory growth, as well as attempted regeneration of portions of damaged nephrons.

The occasional presence of binucleate cells (Fig. 3) is consistent with previous findings in stem cells (Colter et al., 2001) and in the kidney, particularly in podocytes under pathological conditions (Nagata et al., 1995). Whether the binuclearity, wherever observed, is a phenomenon of cell fusion (Humphreys and Bonventre, 2008) or a product of karyokinesis without cytokinesis (Nagata et al., 1995) is unknown, though it suggests a relationship to the generation of daughter-cell pairs.

The combination of NBT perfusion to generate cytoplasmic diformazan with vimentin staining has proven a useful technique for identification of the cells. It is these S3 cells, exclusively, that can exhibit both diformazan precipitation and staining for multiple antigens

(see Table 1). In the presence of a reducing environment, such as would exist in regions where there is cellular production of reactive oxygen species (including superoxide), NBT gains hydrogen and precipitates *in situ* as blue particles of diformazan. Our own observations in normal mouse kidney that has been perfused *in vivo* with NBT demonstrated that there is preferential deposition of diformazan around those nephron components possessing the most mitochondria, namely the S1 segment of proximal tubular epithelial cells (and similar cells that form part of the glomerular capsule: Forbes et al., 2013). The association of mitochondrial activity and NBT staining is strengthened by the intense deposition of diformazan in many of the mitochondrion-rich S3 segment cells.

In the pars recta, a collection of diverse immunoreactive species has been detected in the mitochondrion-rich cells, among them vimentin, CD-44 (also a marker for STCs: Berger et al., 2014), LSD-1, renin, iNOS, Notch1 and Notch2, ferroportin and nitrotyrosine (see Table 1 for complete list), staining for which is absent from adjacent, diformazan-negative epithelial cells. Notably absent from this list are two closely-allied proteins, α-SMA and transgelin, which we have found in kidney epithelium undergoing rapid shape changes, including the glomerulotubular atrophy and scission that occurs in UUO (Forbes et al., 2011) and formation of the cystinotic swan-neck lesions, in which the proximal tubular epithelial cells become severely flattened (Galarreta et al., 2015). The absence of transgelin and α-SMA in mitochondrion-rich S3 tubule cells is confirmed by ultrastructural examination, which found a lack of cytoplasmic filaments.

The occurrence of diformazan-positive cells in the interstitium—some apposed closely to the perimeters of pars recta profiles and penetrating into them (Fig. 7) suggests that at least some of these peculiar cells can migrate into the tubules to augment the epithelial cell population, or perhaps migrate out to augment the interstitial population. Given the various points of origin suggested for stem cells within the kidney (capsule, medulla, tubules), different sources may prove to contribute to nephron elongation when it is required either for normal growth or replacement (Challen et al., 2006).

The regenerative or reparative capability of kidney continues to be a subject of intense interest and study, most of which requires the postulation and identification of stem-like and/or progenitor-like cells that support this process. Whereas extrarenal sources for these cells have frequently been adduced (hematopoietic/bone-marrow-derived), recent experimentation has implicated cells intrinsic to the kidney. Sites suggested for these cells include the capsule (Park et al., 2010), the papilla (Al-Awquati and Oliver, 2006), and the tubules themselves (Humphreys et al., 2008). The so-called “side population” cells of kidney have been shown to be of heterogenous origin (Challen et al., 2006), but appear to be primarily tubule-resident (Maeshima et al., 2003), and several studies implicate the S3 segment of the proximal tubule as a specific niche (Kitamura et al., 2005; Challen et al., 2006; Vogetseder et al., 2007, 2008). That the S3 segment is particularly sensitive to insult is well known (e.g., Venkatachalem et al., 1978; Humphreys and Bonventre, 2008), as well as its cells’ capacity for apparently entering the cell cycle on short notice. It can be debated as to which of these properties is cause, and which result, but apparently this region of the nephron is also provided with especial ability to repair itself, and, presumably, to grow.

The extensive presence, within the mouse kidney pars recta segments, of cells exhibiting features that are frankly atypical of proximal tubule epithelium (small, ovoid, dark nuclei; stellate cell profiles; immunoreactivity against a wide variety of antibodies) appears to belie the assumption that “dedifferentiated” (i.e., e.g., non-columnar) cells are not normally present in mammalian kidney (at least in the mouse). It is curious that these cells have only recently been recognized, in consideration of the extensive use of rodent kidney in renal research. These cells—once highlighted by NBT staining—were found by us to be clearly recognizable in untreated (“normal”) and sham-operated mouse kidneys, as well as being particularly prominent under conditions of ureteral obstruction, as well as found in knockout mice (*Ctns*$^{-/-}$, *eNOS*$^{-/-}$, unpublished observations).

The modern concept of kidney-tubule regeneration gives little credence either to externally-derived stem cells or frankly dedifferentiated, actively mitotic resident tubule cells. Instead it has been proposed that “ordinary” epithelial cells are uniformly capable of division upon demand, and further that the majority of these cells—especially in the S3 segment--chronically exist in a state of regenerative readiness (Witzgall, 2008; Vogetseder et al., 2008). The timing of incorporation and dilution of BrdU, along with presence of mitosis-related antigenic activity such as that of Ki67 and cyclin D1 are adduced as evidence for this “totipotency.” Most often, therefore, the proximal tubule's “straight segment” (S3, pars recta) is implicated both in bearing the primary susceptibility to injury and well as being responsible for principal involvement in the process of restoration.

Most recently the field of study has devolved into two opposing camps, both of which support the concept that tubule repair is dependent upon resident epithelial cells of one sort or another: the one (Romagnani and Kalluri, 2009) proposes a population of specialized stem cells, whereas the other (Humphreys et al., 2011) specifies the contribution of sub-lethally injured (but not specialized) epithelial cells. On the basis of our observations, features of the mouse diformazan-positive S3 segment cells as we have described them may be compatible with both points of view. These include the clear incorporation of the majority of such cells within the proximal-tubule walls under both normal (unoperated/sham-operated) and pathological situations (UUO), the morphology of which suggests a spectrum of differentiation from a primitive form to a mature tubular cell. In addition, their staining against mesenchymal proteins (e.g., vimentin) could be construed as indicative of their existence in a relatively stable state of “epithelial phenotypic change” such as postulated for epithelial cells by Galichon et al. (2013). While not found throughout the entire proximal tubule, the distribution of diformazan-positive cells is more or less random (“stochastic”) within the S3 segment, that portion of the proximal tubule shown to be the most susceptible to damaging conditions.

The studies by Smeets et al. (2013) and Berger et al. (2014) indicate that, in rats and mice, respectively, under normal conditions there is no reserve population of potentially regeneration-supporting cells present, and that these arise only after injury, viz., in the rat obstructed kidney following 7 days of ureteral ligation, but not in its contralateral kidney. Smeets et al. contrast this with the occurrence of similar cells in putatively healthy human kidney, but at the same time point out that their human material may have been compromised to some degree, the normal-appearing tissue having been derived from

kidneys from patients with carcinoma, renal transplantation, or focal segmental glomerulosclerosis.

In this communication, we have sought primarily to document (1) the presence and restricted location of a population of atypical cells within the mouse proximal tubule, (2) a method (NBT perfusion) whereby such cells can be revealed, (3) a consistent pattern of expression of multiple antigens within these cells, and (4) conditions under which these cells are present. Although these cells bear certain resemblances to entities deemed by other investigators to be either stem or precursor cells, further investigation will be required to properly classify them. “Scattered tubular cells” or STCs (Smeets et al., 2013; Berger et al., 2014) and the “proximal tubule rare cells” (PTRCs) reported by Hansson et al. (2014), appear to be identical to one another. Even among the STCs, however, variation in morphology has been reported. While Berger et al. (2014) note in mice with ischemia-reperfusion injury that, while STCs in the affected kidneys lose their brush borders, the borders were retained in STCs of the contralateral control kidneys. In human STCs, by comparison, TEM examination revealed a general absence or reduction of apical microvilli (Smeets et al., 2013; Hansson et al., 2014). In both rat and human, STCs share the property of distribution throughout the proximal tubule and the possession of a sparse mitochondrial complement. In contrast, as summarized in Table 2, the diformazan-positive cells we report here are limited in occurrence to the S3 segment and are present under normal conditions. Importantly, they have a substantial mitochondrial complement, and appear to undergo progressive differentiation to become definitive proximal tubular epithelial cells.

That mitochondrion-rich S3 segment cells have not been previously reported in mice deserves further consideration. In particular, strain differences may be found to play a role. In a study of several strains of mouse, Yabuki et al. (2001) noted the presence, specifically in the S3 epithelium of proximal tubules, of prominent basophilic bodies that proved upon TEM inspection to be huge lysosomes. These were largely limited in occurrence to female animals, and were absent altogether from either sex of C57BL/6 mice, to which strain our present study was limited. Thus it will be of interest to examine other of the commonly-utilized strains of mouse (ICR, BALB/c, etc.), as well as both sexes of each strain, to determine the presence or absence of mitochondrion-rich diformazan-positive S3 segment cells.

Even though the distinct differences mentioned above exist, these should not necessarily disqualify the cells from constituting a subpopulation of STCs. A more unifying view would be to postulate that, in mammalian kidney in general, there exists some population of proximal-cell cells which, though varying in morphological aspects because of (e.g.) certain physiological states, acts to subserve nephron growth and regeneration. We feel that the primary importance of the discovery--now in three mammalian species thus far--of potential tubule-cell progenitors that heretofore have “hidden in plain sight” should be the impetus for further, dedicated attention to be paid to the mammalian kidney—particularly that of human—in order to “resolve the riddle of tubular regeneration.”

ACKNOWLEDGMENTS

Supported in part by the Pediatric Center of Excellence in Nephrology, P50DK096373 from the National Institutes of Health. Technical assistance was provided by Akif Shameem. Particular thanks go to Dr. Stacey Guillot of the University of Virginia Advanced Microscopy Center for her assistance in performing the transmission electron microscopy.

Abbreviations used

NBT	nitroblue tetrazolium
UUO	unilateral ureteral obstruction

REFERENCES

Al-Awqati Q, Oliver JA. The kidney papilla is a stem cells niche. Stem Cell Reviews. 2006; 2:181–184. [PubMed: 17625254]

Berger K, Bangen J-M, Hammerich L, Liedtke C, Floege J, Smeets B, Moeller MJ. Origin of regenerating tubular cells after acute kidney injury. PNAS. 2014; 111:1533–1538. [PubMed: 24474779]

Birn H, Willnow TE, Nielsen R, Norden AGW, Bönsch C, Moestrup SK, Nexø E, Christensen EI. Megalin is essential for renal proximal tubule reabsorption and accumulation of transcobalamin-B_{12}. Am J Physiol Renal Physiol. 2002; 282:F408–F416. [PubMed: 11832420]

Challen GA, Bertoncello I, Deane JA, Ricardo SD, Little MH. Kidney side population reveals multilineage potential and renal functional capacity but also cellular heterogeneity. J. Am. Soc. Nephrol. 2006; 17:1896–1912. [PubMed: 16707564]

Chawla LS, Eggers PW, Star RA, Kimmel PL. Acute kidney injury and chronic kidney disease as interconnected syndromes. N Engl J Med. 2014; 371:58–66. [PubMed: 24988558]

Chevalier RL, Forbes MS, Thornhill BA. Ureteral obstruction as a mocel of renal interstitial fibrosis and obstructive nephropathy. Kidney Intl. 2009; 2009:1145–1152.

Chien C-T, Lee P-H, Chen C-F, Ma M-C, Lai M-K, Hsu S-M. De novo demonstration and co-localization of free-radical production and apoptosis formation in rat kidney subjected to ischemia/reperfusion. J Am Soc Nephrol. 2001; 12:973–982. [PubMed: 11316856]

Colter DC, Sekiya I, Prockop DJ. Identification of a subpopulation of rapidly self-renewing and multipotential adult stem cells in colonies of human marrow stromal cells. Proc Nat Acad Sci. 2001; 98:7841–7845. [PubMed: 11427725]

Duffield JS, Humphreys BD. Origin of new cells in the adult kidney: results from genetic labeling techniques. Kidney Intl. 2011; 79:494–501.

Forbes MS, Ghribi O, Herman MM, Savory J. Aluminum-induced dendritic pathology revisited: cytochemical and electron microscopic studies of rabbit cortical pyramidal neurons. Ann Clin & Lab Sci. 2002; 32:75–86. [PubMed: 11848622]

Forbes MS, Thornhill BA, Chevalier RL. Proximal tubular injury and rapid formation of atubular glomeruli in mice with unilateral ureteral obstruction: a new look at an old model. Am J Physiol Renal Physiology. 2011; 301:F110–F117.

Forbes MS, Thornhill BA, Galarreta CI, Minor JJ, Gordon KA, Chevalier RL. Chronic unilateral ureteral obstruction in the neonatal mouse delays maturation of both kidneys and leads to late formation of atubular glomeruli. Am J Physiol Renal Physiol. 2013; 305:F1736–1746. 2013. [PubMed: 24107422]

Fujigaki Y, Sakakima M, Sun Y, Fujikura T, Tsuji T, Yasuda H, Hishida A. Cell division and phenotypic regression of proximal tubular cells in response to uranyl acetate insult in rats. Nephrol Dial Transplant. 2009; 24:2686–2692. [PubMed: 19395729]

Galarreta CI, Forbes MS, Thornhill BA, Antignac C, Gubler M-C, Nevo N, Murphy MP, Chevalier RL. The swan-neck lesion: proximal tubular adaptation to oxidative stress in nephropathic cystinosis. Am J Physiol Renal Physiol. 2015 doi: 10.1152/ajprenal.00591.2014.

Galichon P, Finianos S, Hertig A. EMT-MET in renal disease: should we curb our enthusiasm? Cancer Letters. 2013; 341:24–29. 2013. [PubMed: 23612071]

Hanae T, Usuda N, Morita T, Nagata T. Light microscopic lectin histochemistry in aging mouse kidney: study of compositional changes in glycoconjugates. J Histochem Cytochem. 1994; 42:897–906. [PubMed: 8014473]

Hansson J, Hultenby K, Cramnert C, Pontén F, Jansson H, Lindgren D, Axelson H, Johansson ME. Evidence for a morphologically distinct and functionally robust cell type in the proximal tubules of human kidney. Hum Pathol. 2014; 45:382–393. [PubMed: 24439225]

Humphreys BD, Bonventre JV. Mesenchymal stem cells in acute kidney injury. Annu Rev Med. 2008; 59:311–325. [PubMed: 17914926]

Humphreys BD, Valerius MT, Kobayashi A, Mugford JW, Soeung S, Duffield JS, McMahon AP, Bonventre JV. Intrinsic epithelial cells repair the kidney after injury. Cell Stem Cell. 2008; 2:284–291. [PubMed: 18371453]

Humphreys BD, Czerniak S, DiRocco DP, Hasnain W, Cheema R, Bonventre JV. Repair of injured proximal tubule does not involve specialized progenitors. Proc Nat Acad Sci. 2011; 108:9226–9231. [PubMed: 21576461]

Kitamura S Yamasaki Y, Kinomura M Sugaya T, Sugiyama H, Maeshima Y, Makino H. Establishment and characterization of renal progenitor like cells from S3 segment of nephron in rat adult kidney. FASEB J. 2005; 19:1789–1797. [PubMed: 16260649]

Maeshima A, Yamashita S, Nojima Y. Identification of renal progenitor-like tubular cells that participate in the regeneration processes of the kidney. J Am Soc Nephrol. 2003; 14:3138–3146. [PubMed: 14638912]

Mahadevappa R, Nielsen R, Christensen EI, Birn H. Megalin in acute kidney injury—foe and friend. Am J Physiol Renal Physiol. 2013; 306:F147–F154. [PubMed: 24197071]

Nagai J, Christensen EI, Morris SM, Willnow TE, Cooper JA, Nielsen R. Mutually dependent localization of megalin and DAB2 in the renal proximal tubule. Am J Physiol Renal Physiol. 2005; 289:F569–F576. [PubMed: 15870384]

Nagata M, Yamaguchi Y, Komatsu Y, Ito K. Mitosis and the presence of binucleate cells among glomerular podocytes in diseased human kidney. Nephron. 1995; 70:68–71. [PubMed: 7617119]

Park H-C, Yasuda K, Kuo M-C, Ni J, Ratliff B, Chander P, Goligorsky MS. Renal capsule as a stem cell niche. Am J Physiol Renal Physiol. 2010; 298:F1254–F1262. [PubMed: 20200095]

Picard N, Baum O, Vogetseder A, Kaissling B, Le Hir M. Origin of renal myofibroblasts in the model of unilateral ureter obstruction in the rat. Histochem Cell Biol. 2008; 130:141–155. [PubMed: 18449560]

Romagnani P. Of mice and men: the riddle of tubular regeneration. J Pathol. 2013; 229:641–644. [PubMed: 23299489]

Romagnani P, Kalluri R. Possible mechanisms of kidney repair. Fibrogenesis & Tissue Repair. 2009; 2:1–10. [PubMed: 19183465]

Smeets B, Boor P, Dijkman H, Sharma SV, Jirak P, Mooren F, Berger K, Bornemann J, Gelman IH, Floege J, van der Vlag J, Wetzels JFM, Moeller MJ. Proximal tubular cells contain a phenotypically distinct, scattered cell population involved in tubular regeneration. J Pathol. 2013; 229:645–659. [PubMed: 23124355]

Venkatachalam MA, Bernard DB, Donohoe JF, Levinsky NG. Ischemic damage and repair in the rat proximal tubule: differences among the S1, S2, and S3 segments. Kidney Intl. 1978; 14:31–49.

Vogetseder A, Palan T, Bacic D, Kaissling B, Le Hir M. Proximal tubular epithelial cells are generated by division of differentiated cells in the healthy kidney. Am J Physiol Cell Physiol. 2007; 292:C807–C813. [PubMed: 16987990]

Vogetseder A, Picard N, Gaspert A, Walch M, Kaissling B, Le Hir M. Proliferation capacity of the renal proximal tubule involves the bulk of differentiated epithelial cells. Am J Physiol Cell Physiol. 2008; 294:C22–C28. [PubMed: 17913845]

Witzgall R. Are renal proximal tubular epithelial cells constantly prepared for an emergency? Focus on “The proliferation capacity of the renal proximal tubule involves the bulk of differentiated epithelial cells”. Am J Physiol Cell Physiol. 2008; 294:C1–C3. [PubMed: 17942631]

Yabuki A, Suzuki S, Matsumoto M, Nishinakagawa H. Sex and strain differences in the brush border and PAS-positive granules and giant bodies of the mouse S3 segment cells. Exp. Anim. 2001; 50:59–66. [PubMed: 11326424]

Fig. 1. Effects of unilateral ureteral obstruction (UUO) on mouse kidney

Median sagittal sections of adult mouse kidneys, stained with *Lotus tetragonolobus* agglutinin to demonstrate proximal tubules in cortex (papillary collecting ducts are also positive). a, sham-operated; b, contralateral kidney after 14 days of UUO applied to the ipsilateral kidney; c, ipsilateral kidney after 7 days UUO; d, ipsilateral kidney after 14 days UUO. With ureteral obstruction, proximal-tubule contribution is severely and progressively reduced.

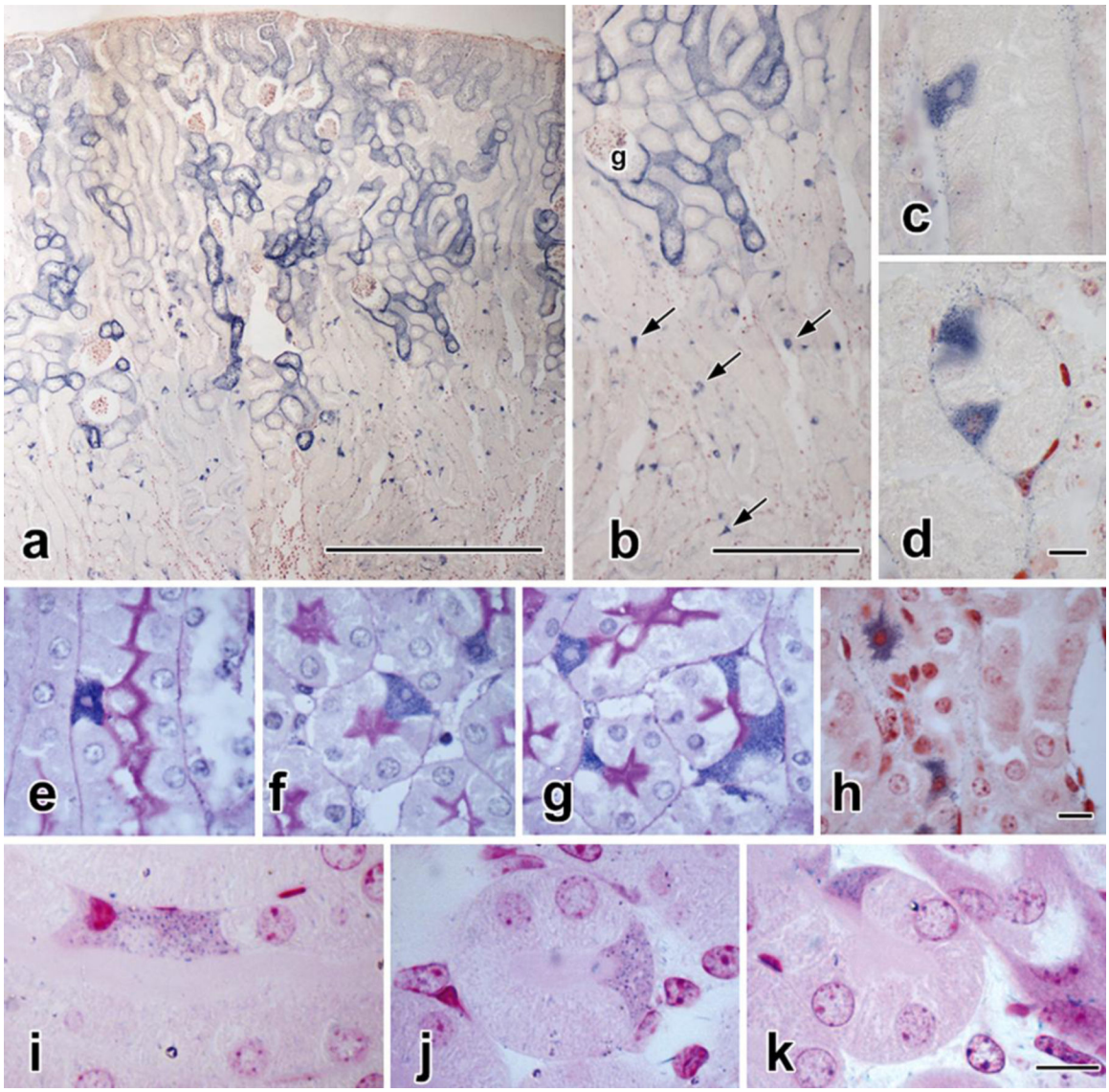

Fig. 2. Nitroblue tetrazolium staining

a-d: Ten-micrometer-thick paraffin section of contralateral kidney from a mouse with 14 days of unilateral ureteral obstruction (UUO).

a. Vascular perfusion with nitroblue tetrazolium (NBT) has resulted in the formation of blue diformazan particles that in the outer cortex outline the S1 and S2 portions of proximal tubules.

b: Detail of a, showing diformazan deposition around the tall epithelial cells of a glomerular capsule (g) and its contiguous proximal tubule. Deeper in the cortex, the S3 (pars recta) segments lack a distinct marginal coating, but instead contain scattered, highly-positive cells (arrows).

c, d: Additional details of pars recta tubules, with diformazan-filled cells in longitudinally- (c) and transversely-cut profiles (d).

e-h: Two-micrometer paraffin sections of 14-day UUO contralateral kidney, NBT-perfused. e, f, g. PAS-hematoxylin staining; h, Neutral Red counterstaining. The cells in the pars recta

derive their distinct blue coloration from cytoplasmic deposits of diformazan crystals; their morphology differs from neighboring proximal-tubule epithelial cells in the size, shape, and density of their nuclei, as do their overall profiles ranging from triangular (f, g), to stellate (h).

i-k: “Semithin” (ca. 0.25 μm) sections of glutaraldehyde-fixed, plastic-embedded (unosmicated) kidney from sham-operated, NBT-perfused mouse, with basic fuchsin counterstaining. In these thinner sections, individual diformazan particles can be resolved against a dark cytoplasmic background.

Scale bar in a = 500 μm; in b = 100 μm; in d = 10 μm and applies to both d and d; in h = 10 μm and applies to e-h, and in k = 10 μm and applies to i-k.

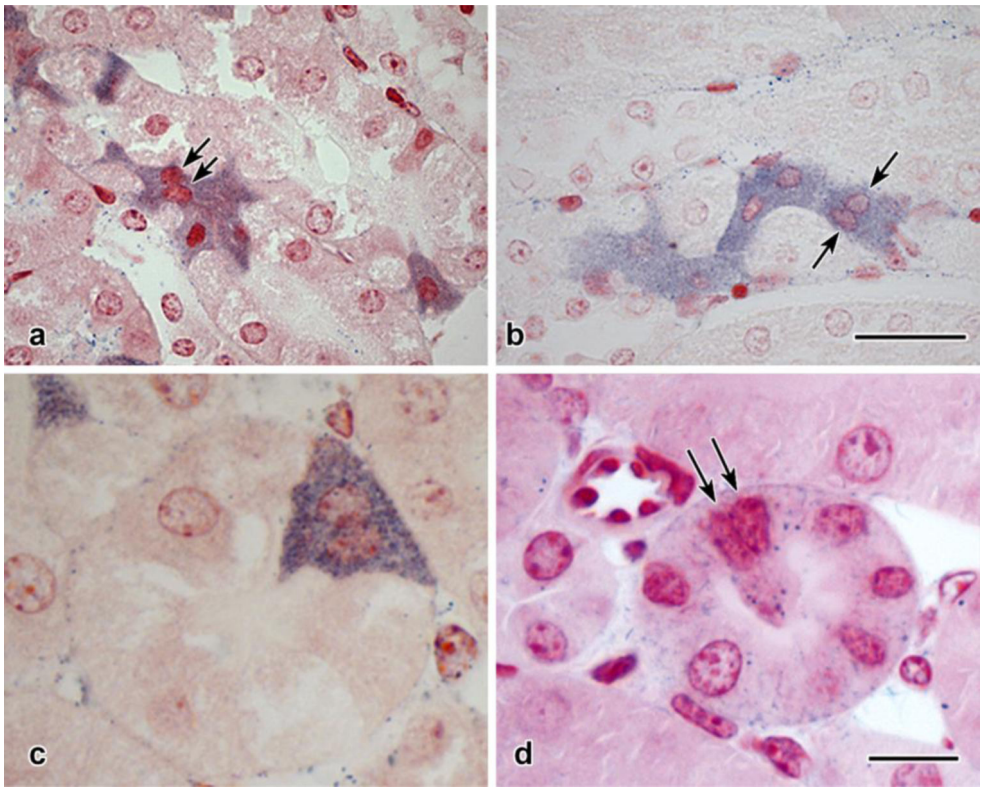

Fig. 3. Configurations of S3 segment proximal tubular cells

a, b: Two-micrometer paraffin sections, NBT-perfused and Neutral Red counterstained. In both micrographs, diformazan-stained cells are found in groups, and in some cases (arrows) doublets of nuclei are closely apposed.

c: Detail of cross-sectioned pars recta tubule. The diformazan-positive profile contains two nuclear profiles.

d: Semithin (<0.25 μm) plastic section, glutaraldehyde-fixed, unosmicated tissue with basic fuchsin counterstaining. A characteristic cell is identifiable by the deposition of diformazan particles (cf. Fig. 2 i-k), and a doublet of nuclei, similar to that seen in c, is visible within its confines (arrows).

Scale bar in b = 25 μm and applies to a and b; scale bar in d = 10 μm and applies to c and d.

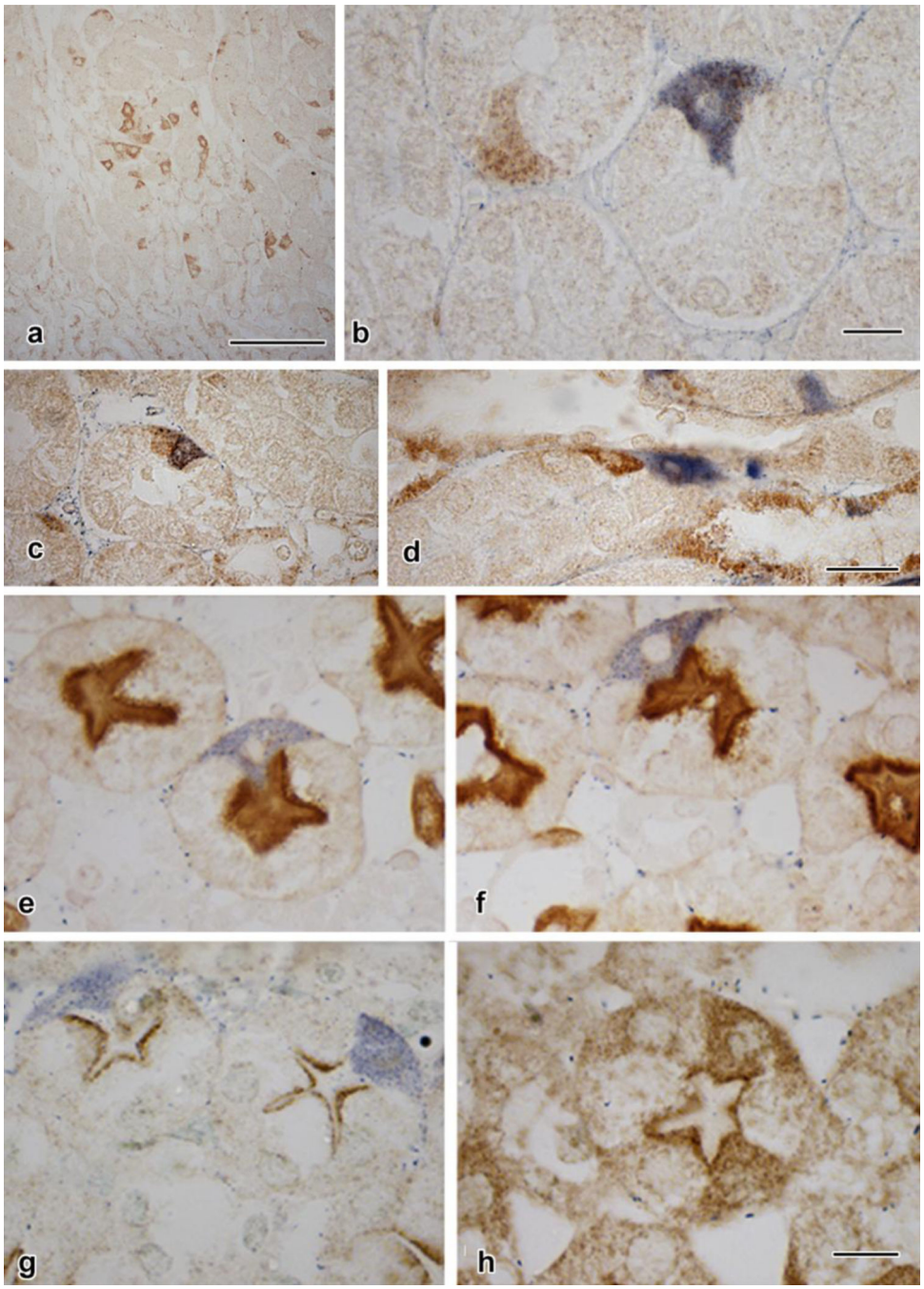

Fig. 4. Immunostaining in diformazan-positive S3 segment proximal tubular cells

a: Untreated mouse (no surgery, no NBT exposure, no counterstaining). Multiple vimentin-positive cells, their sizes, shapes, and location in pars recta identifying them as identical to the pleiomorphic cells shown in Fig. 2.

b-d: Fourteen-day UUO, contralateral kidney. In b, adjacent pars recta tubules contain pleiomorphic cells, one vimentin-positive but lacking diformazan precipitate, the other positive for both stains.

c, d: Doublets of pars recta cells. In each pair, one cell is positive for vimentin, whereas the other contains only diformazan particles.
e-h: Two-micrometer-thick paraffin sections (e-f and g-h, each set taken from the same section, demonstrating the variety of forms and staining properties of cells).
e, f: *Lotus tetragonolobus* agglutinin staining, which specifically concentrates at the apices of typical proximal tubule epithelial cells, forming a dark line just below the more lightly-staining brush border, the line corresponding to the apical tubulovesicular ("endocytic") system, which is rich in α-L-fucose to which the agglutinin is attracted. In some examples (e), the blue diformazan-stained cell lacks apical staining, whereas apical positivity is evident in the profile shown in f.
g, h: Immunostaining for megalin, a receptor specific to the proximal-tubule tubulovesicular system. In g, the cells are devoid of megalin positivity, each presenting an unmarked apex. In h, megalin positivity appears in the cytoplasts and an apical concentration is seen.
Scale bar in a = 100 μm; in b =10 μm; in d = 25 μm and applies to c and d; in h = 10 μm and applies to g and h.

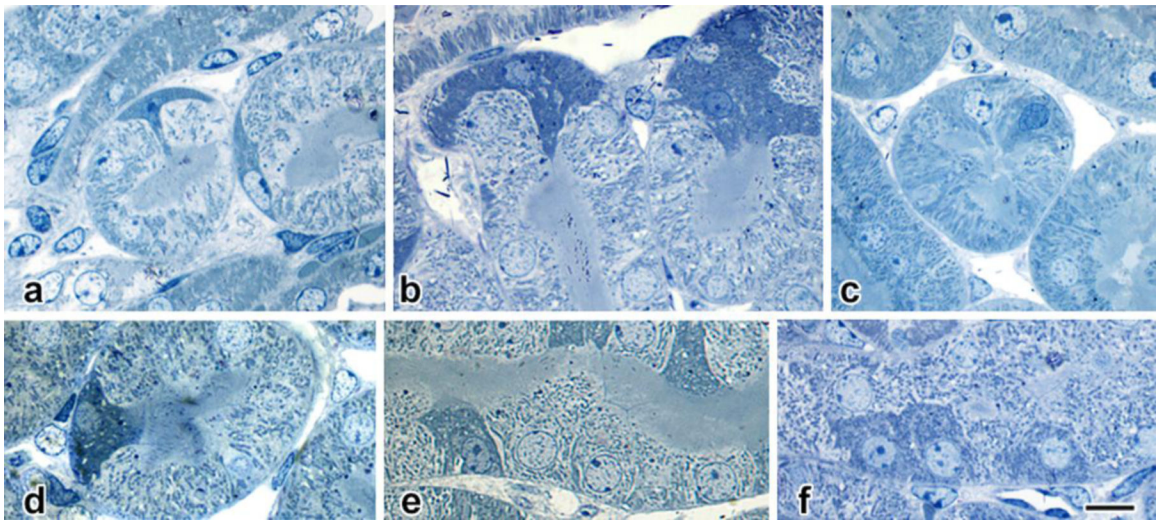

Fig. 5. Structural details in semithin (<0.25 μm) plastic sections of glutaraldehydeperfused kidney

In the same animal (42-day sham-operated male mouse), a spectrum of morphologies is found, ranging from seemingly surface-applied cells with cytoplasmic processes projecting inward between normal epithelial cells (a, b) to cells with dark nuclei (c, d) and profiles that occupy the full depth of the tubule wall, to cells with larger nuclei (e, f) that more closely resembling those of their neighbors, but retaining their cytoplasmic osmiophilia. Scale bar in f = 10 μm and applies to all panels.

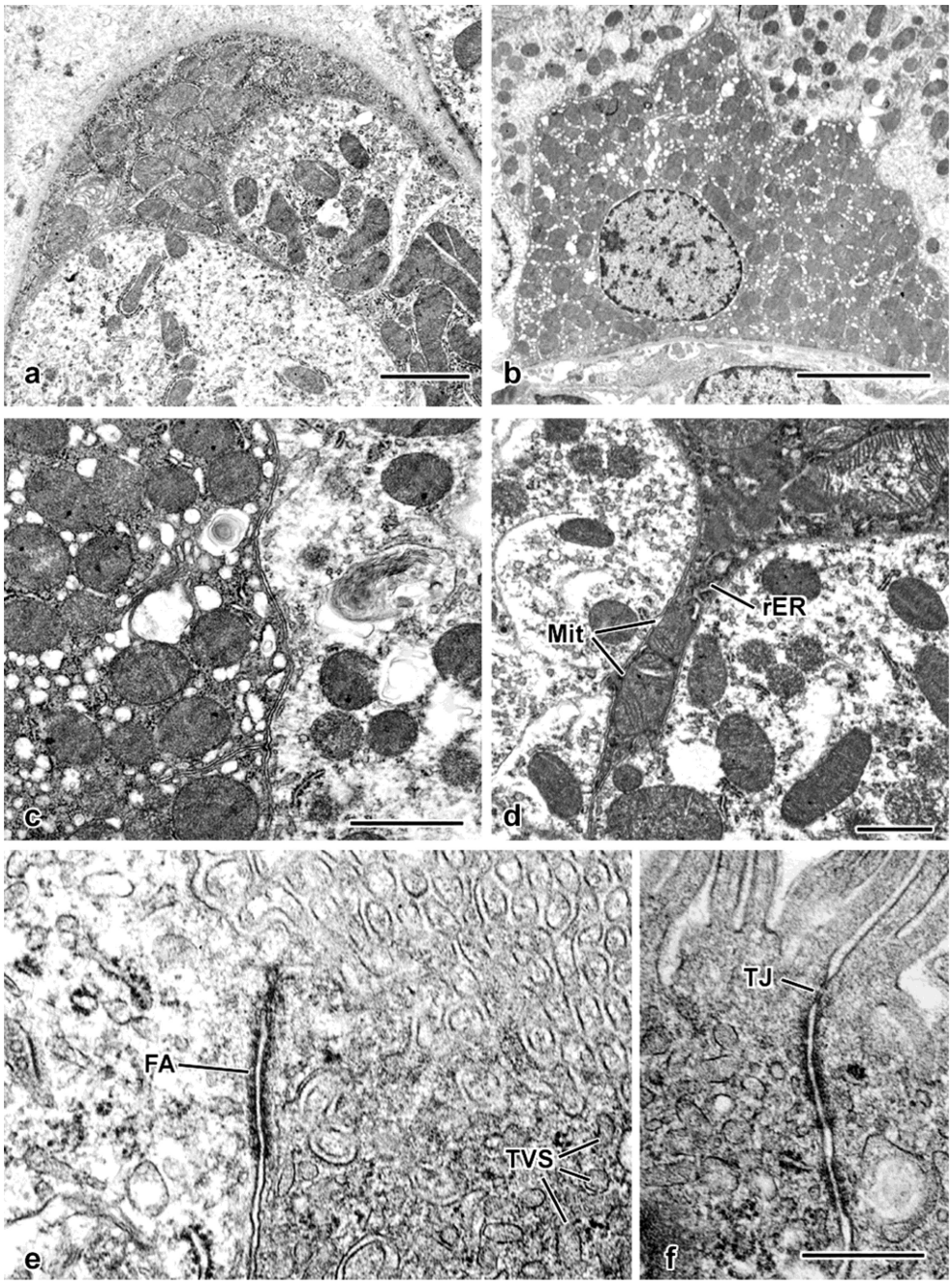

Fig. 6. Fine-structural details of glutaraldehyde-perfused mouse kidney

a. An electron-opaque profile forms part of this tubule's surface (compare with the semithin section image in Fig. 5a). Its cytoplasm is filled with mitochondria.

b. Survey view, showing an ovoid, heterochromatic nucleus and cytoplasmic concentration of mitochondria.

c. Apposition of two S3 epithelial cells, demonstrating higher mitochondrial concentration and ribosome-rich cytoplasm of one (at left) as opposed to an adjacent S3 segment epithelial cell containing scattered mitochondria and electron-lucent cytoplasm typical of the majority of proximal-tubule epithelial cells.

d. Thin cytoplasmic process extending between two proximal tubular epithelial cells. Both mitochondria (Mit) and rough endoplasmic reticulum (rER) are present within the confines of the process.

e. Apical portions of an S3 segment epithelial cell (at left) and a mitochondrion-rich cell (at right), with a prominent “intermediate” junction (fascia adherens: FA) joining the two cells. Both the brush border and tubulovesicular system elements (TVS) are evident.

f. Apical junctional complex formed between two adjoining mitochondrion-rich cells, with both a tight junction (TJ) and adherens junctions.

Scale bar in a = 2 μm; in b = 5 μm; in c = 1 μm; in d = 1 μm; in f = 0.5 μm and applies to e and f.

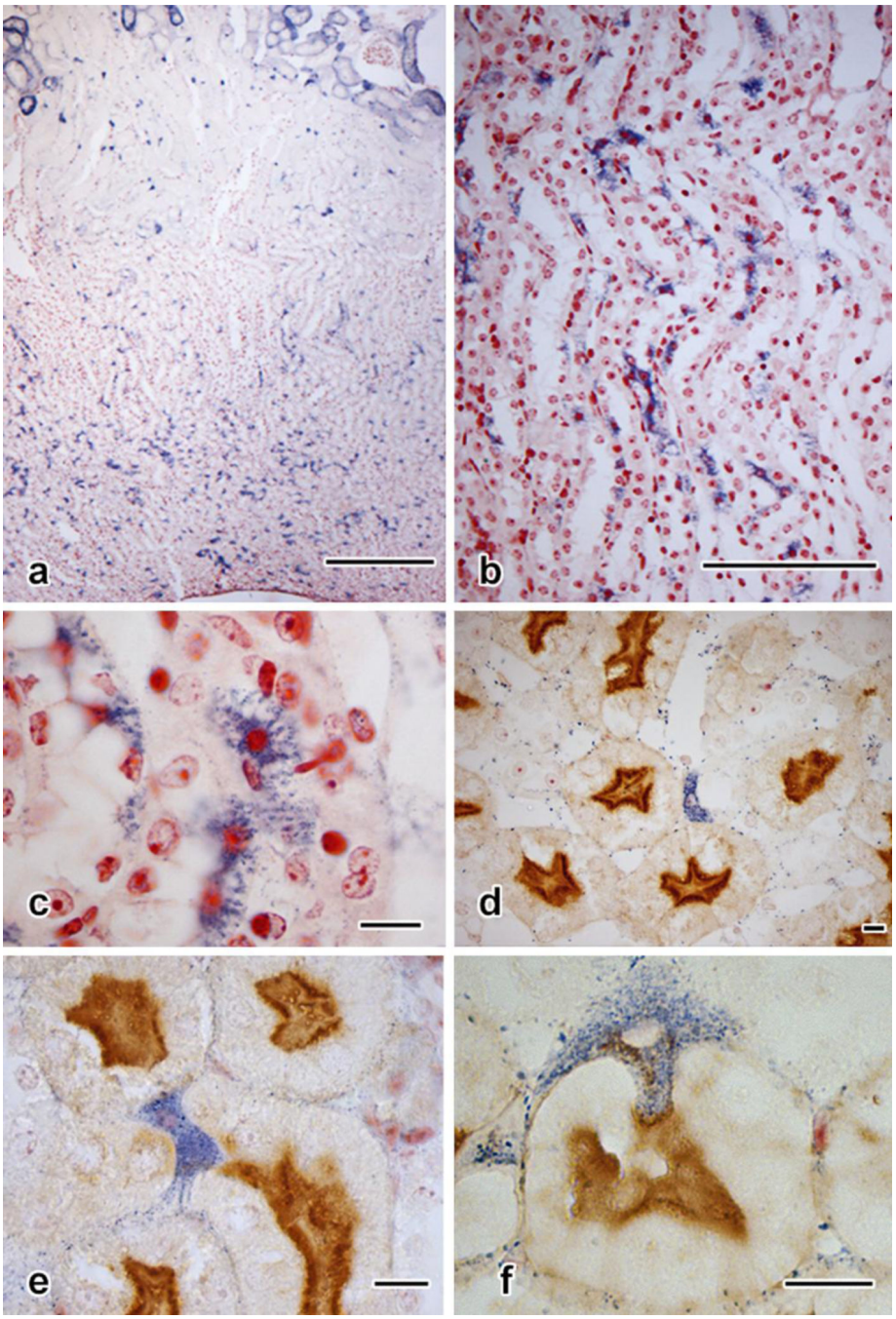

Fig. 7. Extratubular cells positive for NBT reduction

a. Medulla in 10-μm section (cortex shown in Fig. 2a). Multiple diformazan-positive cells are present.

b. Two-micrometer section from medullary region shown in A, showing distribution of cells in the medullary tubules.

c. Detail of b, illustrating the dendritic profiles and densely staining nuclei of diformazan-stained tubule cells.

d. Two-micrometer section (Lotus staining) with a blue cell constituting part of the wall of a portion of the thin loop.
e. Interstitial diformazan-positive cell sandwiched among several pars recta profiles.
f. A diformazan-positive cell appears to adhere to the outer border of a proximal tubule while inserting a cytoplasmic projection into the tubule. Lotus staining with Neutral Red counterstain. Scale bar in a = 250 μm; scale bar in b = 100 μm; scale bars in c-f each =10 μm.

TABLE 1

Staining of Individual Mitochondrion-Rich S3 Segment Proximal Tubular Cells in Adult Mice

Substance	Source	Product No.	Host/MC/PC	Dilution	Positive or Negative
CD-44	Abcam	ab-41478	Rb PC	1:100	+
Cyclin D1	Thermo Scientific	RC-010	Rb PC	1:200	+
E-cadherin	Santa Cruz	sc-7870	Rb PC	1:250	+
Ferroportin	Santa Cruz	sc-49668	Gt PC	1:200	+
Fibronectin	Abcam	ab-6328	Ms MC	1:200	+
4-hydroxy-nonenal	Abcam	ab-48506	Ms MC	1:1000	+
iNOS	Santa Cruz	sc-7271	Ms MC	1:250	+
Ki-67	Abcam	ab-66195	Rb PC	1:250	+
Lotus tetragonolobus agglutinin	Vector Laboratories				± apical cytoplasmic staining
LSD-1	Abcam	ab-17721	Rb PC	1:1500	+
Megalin/Lrp2	Abcam	ab-76969	Rb PC	1:500	± apical cytoplasmic staining
NBT (nitroblue tetrazolium)	Sigma-Aldrich	N5514			+
Notch1	Santa Cruz	sc-9170	Rb PC	1:100	+
Notch2	Santa Cruz	sc-5545	Rb PC	1:100	+
Nitrotyrosine	Millipore	06-284	Rb PC	1:1000	+
Osmication					+
PAS	Electron Microscopy Sciences				Not specific: intrinsically darker cytoplasts
PAX-2	Zymed Labs.	71-6000	Rb PC	1:200	+
Renin	Gift from Dr. Tadashi Inagami Vanderbilt U.		Gt PC	1:10,000	+
Silver methenamine (Jones silver stain)					Nuclei highly argentophilic
α-SMA	Sigma-Aldrich	A-2547	Ms MC	1:800	-
Transgelin	Gift from Dr. ShuMan Fu University of Virginia		Rb PC	1:1500	-
Trichrome	Sigma-Aldrich				+ (again on basis of overall darker cytoplasm)
TUNEL ApopTag®	Millipore	S-7100			-
Vimentin	Abcam	ab-45939	Rb PC	1:2500	+

Abcam/Cambridge, MA

Electron Microscopy Sciences/Hatfield PA

Millipore/Temecula, CA

Polysciences/Warrington, PA

Santa Cruz Biotechnology/Santa Cruz, CA

Sigma-Aldrich/St. Louis, MO

Thermo Scientific/ Suwannee GA

Vector Laboratories/Burlingame, CA

Zymed Laboratories/San Francisco CA

Table 2

Comparison of Atypical Proximal Tubule Epithelial Cells

Term	Location	Species	Vimentin positive?	Brush border?	Mitochondrial Content?	Cytoplasmic Filaments?
PTRCs*	Throughout injured proximal tubule	Human	Y	N	Low	Y
STCs**	Throughout injured proximal tubule	Mouse, Rat	Y	N	Low	Y
	Throughout normal proximal tubule	Human	Y	N	Low	Y
Pars recta mitochondrion-rich cells***	Restricted to S3 portion of normal or injured proximal tubule	Mouse	Y	Y	High	N

* "Proximal tubule rare cells". Hansson et al., 2014

** "Scattered tubular cells". mouse: Berger et al., 2014; human, rat: Smeets et al., 2013

*** present study